

The *elongata* mutants identify a functional Elongator complex in plants with a role in cell proliferation during organ growth

Hilde Nelissen*, Delphine Fleury*, Leonardo Bruno*, Pedro Robles†, Lieven De Veylder*, Jan Traas‡, José Luis Micol†, Marc Van Montagu*, Dirk Inzé*, and Mieke Van Lijsebettens*[§]

*Department of Plant Systems Biology, Flanders Interuniversity Institute for Biotechnology, Ghent University, Technologiepark 927, B-9052 Gent, Belgium;

†División de Genética and Instituto de Bioingeniería, Universidad Miguel Hernández, Campus de Elche, E-03202 Elche, Spain; and ‡Laboratoire de Biologie Cellulaire, Institut National de la Recherche Agronomique, F-78026 Versailles Cedex, France

Contributed by Marc Van Montagu, April 6, 2005

The key enzyme for transcription of protein-encoding genes in eukaryotes is RNA polymerase II (RNAPII). The recruitment of this enzyme during transcription initiation and its passage along the template during transcription elongation is regulated through the association and dissociation of several complexes. Elongator is a histone acetyl transferase complex, consisting of six subunits (ELP1–ELP6), that copurifies with the elongating RNAPII in yeast and humans. We demonstrate that point mutations in three *Arabidopsis thaliana* genes, encoding homologs of the yeast Elongator subunits ELP1, ELP3 (histone acetyl transferase), and ELP4 are responsible for the phenotypes of the *elongata2* (*elo2*), *elo3*, and *elo1* mutants, respectively. The *elo* mutants are characterized by narrow leaves and reduced root growth that results from a decreased cell division rate. Morphological and molecular phenotypes show that the *ELONGATA* (*ELO*) genes function in the same biological process and the epistatic interactions between the *ELO* genes can be explained by the model of complex formation in yeast. Furthermore, the plant Elongator complex is genetically positioned in the process of RNAPII-mediated transcription downstream of Mediator. Our data indicate that the Elongator complex is evolutionarily conserved in structure and function but reveal that the mechanism by which it stimulates cell proliferation is different in yeast and plants.

Arabidopsis | histone acetyl transferase complex | leaf development | RNA polymerase II

Currently, acetylation is the best-characterized histone modification and plays a role in the regulation of transcription (1–3). This reversible modification results from a balance between the activity of histone deacetylases and histone acetyl transferases (HATs). The Elongator complex consists of six subunits, of which one displays HAT activity (4). Elongator copurifies with RNA polymerase II (RNAPII) during transcriptional elongation, presumably by rendering the DNA more accessible for the passage of the polymerase (5, 6). In *Arabidopsis thaliana* (L.) Heyhn., 16 histone deacetylases and 12 HATs are encoded by the genome (7), and mutational analysis has already shown that some of these genes are involved in stress responses, growth, and flower development (8–11).

In a large-scale screening of ethane methylsulfonate-mutagenized *Arabidopsis* for mutants with abnormally shaped leaves, the *elongata* (*elo1*, *elo2*, *elo3*, and *elo4*) mutations have been identified (12) and mapped at low resolution by linkage analysis (13). The *elo* mutants have a narrow leaf phenotype (12), similar to that of the null mutant *drl1-2*. Subsequently, *elo4* was shown to be allelic to *drl1* and was redesignated *drl1-4* (14). DRL1 is the ortholog of the yeast KTI12 protein (14), a putative regulator of the Elongator complex (15). Homologs of the six structural components of Elongator are present in the *Arabidopsis* genome (14). We report that the *elo* mutations are in genes encoding components of the Elongator complex. Pheno-

typical analyses showed that mutations in the plant Elongator HAT and its structural components interfere principally with leaf shape, and leaf and root growth by affecting cell proliferation.

Materials and Methods

Plant Material and Growth Conditions. Mutants *elo1*, *elo2*, *elo3*, *elo4/drl1-4* (12), *drl1-2* (code N9360, Nottingham Seed Stock Centre, Nottingham, United Kingdom) (14), and *swp1* (16) have been described previously; *elo3-3*, *elo3-4*, and *elo3-5* (The Plant Chromatin Database available at www.chromdb.org), *elo3-2* (FLAGdb/FST) (17), and SALK insertion lines (Nottingham Seed Stock Centre) are publicly available. Plants were grown as described in ref. 14. For transcript profiling experiments, the medium was 2.15 g/liter Murashige and Skoog medium salts (Duchefa, Haarlem, The Netherlands)/1 g/liter sucrose/0.5 g/liter Mes, pH 6.0/6 g/liter plant tissue culture agar. Seeds were vernalized for 3 days after sowing.

Morphological and Cellular Analysis. Morphological, cellular, and statistical analyses were performed on the expanded first two leaves of the Elongator mutants [35 days after germination (DAG)] and *Ler* (28 DAG) as described in ref. 18. Seeds were germinated *in vitro* on vertical plates; every 2 days, primary root growth was measured. An analysis of variance was performed on each double mutant (DM), its respective parents, and *Ler*, with the two mutated genes as fixed factors and the slope of root growth as a variable ($n = 10$). A significant interaction between the two loci showed an epistatic effect between the genes.

Leaf primordia of 7-DAG *Ler*, *elo1*, *elo2*, *elo4/drl1-4*, and *drl1-2* plants ($n \geq 7$) were analyzed (19). The distance between 10 neighboring nuclei was measured (five times per primordia) to account for errors on the measurements.

Flow Cytometry Analysis of the Leaves. The *elo* and *drl* mutants have delayed development after germination, and growth is very heterogeneous among individuals; therefore, the first two leaves of the mutants and *Ler* were harvested according to developmental stages (1.02, 1.03, etc.) (20). In wild-type plants, three successive phases could be determined during leaf development: proliferation (mitotic cell cycles, illustrated by the presence of

Abbreviations: AFLP, amplified fragment-length; DAG, days after germination; DE, differentially expressed; DM, double mutant; HAT, histone acetyl transferase; RNAPII, RNA polymerase II.

Data deposition: The microarray data reported in this paper have been deposited in the ArrayExpress database (accession no. E-MEXP-300), and the sequences reported in this paper have been deposited in the European Molecular Biology Laboratory database (accession nos. AJ964957 and AJ964958 for ELO1 and ELO3, respectively).

[§]To whom correspondence should be addressed. E-mail: mieke.vanlijsebettens@psb.ugent.be.

© 2005 by The National Academy of Sciences of the USA

Table 1. Alleles of the *ELO2*, *ELO3*, and *ELO1* genes

Locus	MIPS	Allele	Ecotype	Mutagen	Source
<i>ELO2</i>	At5g13680	<i>elo2 = elo2-1</i>	Ler	EMS	12
		<i>elo2-2</i>	Col-0	T-DNA	29
		<i>elo2-3</i>	Col-0	T-DNA	29
<i>ELO3</i>	At5g50320	<i>elo3 = elo3-1</i>	Ler	EMS	12
		<i>elo3-2</i>	Ws-2	T-DNA	16
		<i>elo3-3</i>	Ws-2	RNAi	ChromDB
		<i>elo3-4</i>	Ws-2	RNAi	ChromDB
		<i>elo3-5</i>	Ws-2	RNAi	ChromDB
<i>ELO1</i>	At3g11220	<i>elo1 = elo1-1</i>	Ler	EMS	12
		<i>elo1-2</i>	Col-0	T-DNA	29
		<i>elo1-3</i>	Col-0	T-DNA	29

RNAi, RNA interference; EMS, ethane methylsulfonate; MIPS, Munich Information Center for Protein Sequences; ChromDB, Plant Chromatin Database.

three independent RNA interference lines of *ELO3* (N3981, N3982, and N3983) in Wassilewskija (*Ws-2*) ecotype had leaf and root phenotypes (see below) very similar to those of the *elo* mutants (Table 1).

The Functional Domains of the Elongator Proteins Are Evolutionarily Conserved. An *in silico* analysis showed that the functional domains of the *ELO2*, *ELO3*, and *ELO1* proteins were conserved between yeast and *Arabidopsis*. In yeast, the Elongator complex consists of two distinct subcomplexes. ELP1 was previously described as part of the core subcomplex of Elongator where it functions as a scaffold protein to form a “bridge” between the two subcomplexes (4). Alignments of the homologs (from eight species) with the *Arabidopsis* *ELO2* protein revealed conserved domains that were also present in other scaffold protein families, such as the 14-3-3 proteins, supporting a putative role for *ELO2* in stabilizing the interaction between different components of the Elongator complex. The *elo2* mutation is predicted to form a truncated protein that does not contain a conserved C-terminal domain. The yeast ELP3 protein was reported to possess HAT activity *in vitro* (30). By sequence analysis, the ELP3 HAT was classified in the GCN5-related *N*-acetyltransferase superfamily (7), and a methyltransferase domain was found as well (31). The presence of a GCN5-related *N*-acetyltransferase family domain (accession no. PF00583) and a radical *S*-adenosyl methionine superfamily domain (accession no. PF04055) imply a similar functionality of *ELO3* in *Arabidopsis*. The HAT and methyltransferase domains of *ELO3* suggested that this protein might be the key enzyme of the Elongator complex because it would render the chromatin more accessible for the passage of the RNAPII transcription machinery by modifying histones. In the *elo3* mutants, an aspartic acid residue, which is conserved in all *ELO3* homologs (from >32 species) within the HAT domain, is converted to an asparagine. The extreme phenotype of the *elo3* mutants, compared with the other *elo* mutants, demonstrated the importance of this aspartic acid for the functionality of the *ELO3* protein. The yeast ELP4, which forms the accessory subcomplex with ELP5 and ELP6, has been reported to be an inactive ATPase homolog (32). By using the *Arabidopsis* *ELO1* protein, we identified a RecA domain (accession no. PS00321) at the N-terminal region of the protein. The RecA motif was first identified in bacterial recombinases and is also present in the eukaryotic Rad51 and DMC1 proteins (33). However, because neither the recombinase (accession no. PS00674) nor the ATP-binding signatures are present in the *Arabidopsis* *ELO1* protein, *ELO1* is probably not a recombinase *sensu strictu*. The sequence similarity between *ELO1* and the recombinase superfamily of ATPases indicates that *ELO1* might represent a previously uncharacterized type of DNA binding/processing protein. The *elo1* mu-

tation is predicted to cause truncation of the moderately conserved C-terminal part of the *ELO1* protein.

The expression of the *ELO1*, *ELO2*, and *ELO3* genes was monitored in different plant organs by RT-PCR: roots, young first leaves, whole seedlings (14 DAG), cotyledons, expanded first leaves, floral buds, and shoot apices (27 DAG). The three *ELO* genes were expressed in every plant organ examined (data not shown) in the same manner as the *DRL1* gene (14). These expression data were confirmed *in silico* for each organ at different developmental stages by using the Genevestigator database (34).

Reduced Organ Growth Phenotype. Although the *elo* mutants were originally isolated as leaf mutants (12), they all displayed a pleiotropic phenotype: The growth of the primary roots was reduced, and the architecture of the inflorescences was altered and reduced in length compared with wild type. Furthermore, upon germination, seedling growth was delayed in all *elo* mutants and germination was severely retarded in *elo3*. The phenotypes of the different *elo* mutants were very similar and resembled that of *drl1-2* (Fig. 1D). However, quantification of some of the phenotypes resulted in differences in phenotypic severity between the different *elo* and *drl* mutants. Fully expanded first and second leaves collected 28 DAG were analyzed for a number of parameters (18). The lamina, petiole, and total leaf length were increased significantly in *elo1*, *elo2*, and *elo4/drl1-4* compared with *Ler* ($n \geq 10$), and the transition between lamina and petiole was unclear. The lamina width was smaller in all mutants because of a reduced cell number as measured by the number of palisade cells (Fig. 2B). *elo3* displayed the most severe phenotype, with a 52.4% reduction in palisade cell number (Fig. 2A and B). In *elo4/drl1-4*, the cell number was not significantly reduced (Fig. 2B), confirming that it was a weak allele of *DRL1* (14). In transverse sections through first and second fully expanded *elo3* leaves, larger and more irregularly shaped palisade cells, more intercellular spaces, and normal vascular bundles with dorsal xylem and ventral phloem tissue were seen, a leaf anatomy reminiscent of that of *drl1-2* (Fig. 2A) (14). In conclusion, the narrow leaf phenotype of *elo* mutants was very similar to that of the *drl1-2* mutant (14) and was also associated with a reduction in cell number.

Kinetics of primary root growth was measured in *elo1*, *elo2*, *elo3*, *drl1-2*, and *elo4/drl1-4* homozygotes and compared with the wild-type *Ler* ($n \geq 10$). Root growth was significantly inhibited in all mutants (Fig. 2C). Statistical analysis positioned each of the mutants in a distinct group, except for the *drl1-2* and *elo2* mutants that formed one group, based on their root growth (Fig. 2C). Other alleles of *ELO3* (*elo3-2*, *elo3-3*, *elo3-4*, and *elo3-5*) also showed retarded root growth compared with that of *Ws-2* ($n \geq 10$) (Fig. 5A, which is published as supporting information on the PNAS web site). The growth rate of the primary roots was calculated as root length difference between two successive time points divided by the time interval between these time points. The growth rate of the last time points was used to determine cell production in the roots, which was a measure for the number of cells produced per hour and is the ratio of the root growth rate and the length of the mature root cortex cells. The length of the mature cortex cells was significantly shorter in all *elo* and *drl1-2* mutants (data not shown), and cell production was severely decreased in the mutant root (Fig. 2D). The phenotypic analyses of the Elongator mutants showed that the Elongator genes have a positive effect on lateral leaf and primary root growth, which coincides with their expression in these organs. The similar phenotypes of the different Elongator mutants suggest that the Elongator genes play a role in the same pathway, process, or even in the same complex, as previously shown for mutants with similar developmental phenotypes, such as the *clavata* mutants (35). Comparable phenotypes were obtained upon mutation of *ELO3*, the putative HAT, *DRL1*, a putative regulator, and the structural components *ELO2* and *ELO1*, implying that each component examined was important for the functionality of Elongator in plants.

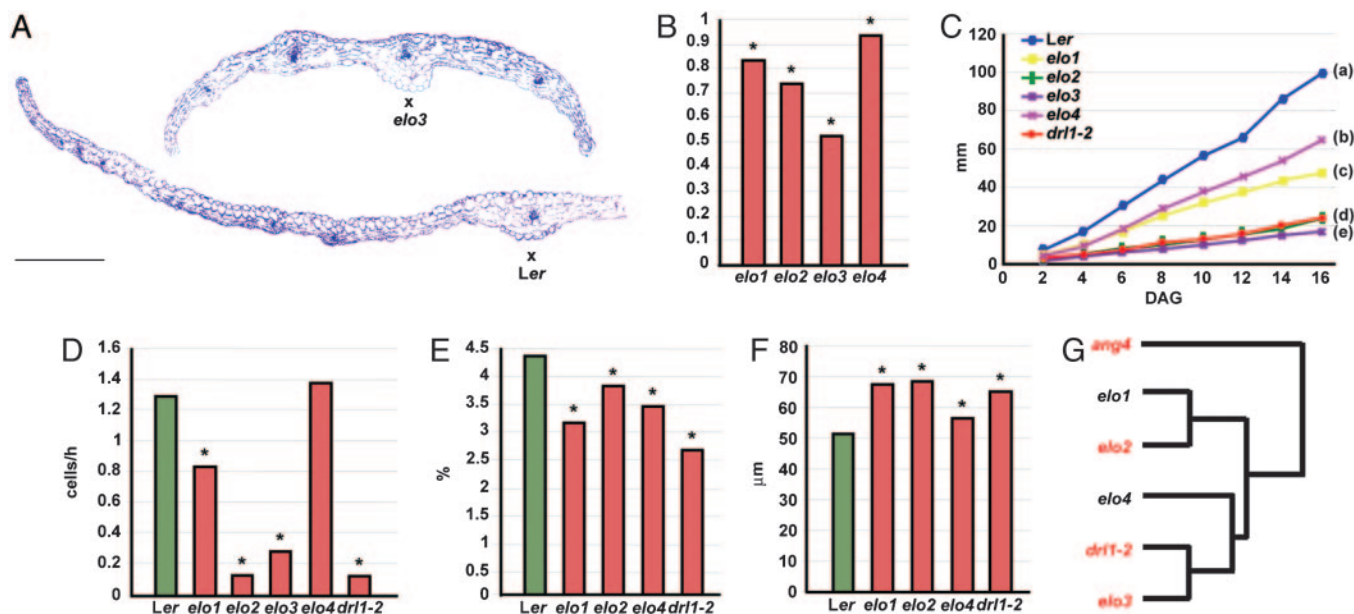


Fig. 2. Morphological and molecular phenotyping of the *elo* and *drl* mutants. (A) Sections of fully expanded first leaves (28 DAG) at the widest point of *elo3* and of *Ler*. *, Midveins. (Bar, 0.5 mm.) (B) Number of palisade cells at the widest point of fully expanded leaves of *elo1*, *elo3*, *elo2*, and *elo4/drl1-4* in proportion to *Ler* (arbitrary indicated as 1). (C) Primary root growth kinetics of *elo1*, *elo2*, *elo3*, *elo4/drl1-4*, *drl1-2*, and *Ler*. A pairwise multiple-testing analysis positions the lines in groups a to e. (D) Cell production in the roots of *elo1*, *elo2*, *elo3*, *elo4/drl1-4*, *drl1-2*, and *Ler*. (E) Mitotic index of the leaf primordia (7 DAG). (F) Cell size in the leaf primordia (7 DAG). (B–F) *, Significant differences between wild type and mutants according to a *t* test ($P < 0.05$). (G) Complete linkage hierarchical clustering of narrow leaf mutants for 763 cDNA-AFLP DE genes at a significant level ($P \leq 0.001$). The same clustering position was found with 2,897 DE genes between mutant and *Ler* in the microarray experiment for the genotypes in red. The data used are \log_2 -transformed ratios between mutant and wild type.

The *elo* Mutants Have a Reduced Cell Proliferation Rate, Probably Without Affecting the Core Cell Cycle Machinery. The serious delay in growth after germination and the reduced cell numbers underlying the *elo* and *drl* phenotypes suggest a decrease in cell division rate. Cell division activity is also decreased in the yeast Elongator mutants; the cells undergo a G_1 delay and are often not able to continue the cell cycle (36). Several observations support a change in the cell division rate for the Elongator mutant plants: The mitotic index was significantly lower in the mutant primordia 7 DAG (Fig. 2E), implying that the duration of interphase was prolonged over that of mitosis (37). Moreover, the distance between the nuclei, which is a direct measure of cell size (19), was significantly higher in the *elo* mutants, and the cells were larger (Fig. 2F). This observation is in agreement with a decrease in cell division rate, because cell size is negatively correlated with cell division rate, as observed for the lines overexpressing *E2Fa/DPa* and Kip-related proteins (22, 38). Previously, an altered cell division rate in the leaf primordia was shown to have a serious impact on leaf morphogenesis (39).

To assess whether the reduced cell division rate upon mutation of the Elongator complex was also due to a G_1 delay in plants, the ploidy levels were measured by flow cytometry in the first two leaves of mutants and wild-type plants at several time points during development. In contrast to yeast, no shift in the G_1 -to- G_2 populations could be determined at the first time points (66.21% 2C and 33.79% 4C in *Ler*; 62.44% 2C and 31.37% 4C in *elo3*; Fig. 5B and C) in Elongator mutant plants, indicating a similar effect on both the G_1 -to-S and G_2 -to-M transition points of the cell cycle. These data show that the Elongator complex has a positive effect on the cell division rate in yeast and plants, but the mechanism through which this is exerted differs between the two species.

Furthermore, the flow cytometry profiles of the first two leaves also ruled out the possibility that the reduced cell number was due to an early exit from the mitotic cell divisions in the *elo* mutants, because the curves of cells in 2C and 4C intersected around the same developmental time point as in wild type (Fig.

5B and C). When the growth retardation of the *elo* and *drl* mutants is taken into account, the mitotic cell divisions would stop even later than those of the wild type. The differences in endocycling between the mutant and wild-type plants were not significant and could have resulted from differences in age of the seedlings at the time of harvesting. The cell expansion that is correlated to endoreduplication goes on longer in the *elo* mutants, explaining a slightly higher ploidy level in the mutants (Fig. 5B and C). In conclusion, no direct defect was observed on the cell cycle transitions or on the endocycling; therefore, the effect of the *elo* and *drl* mutations on cell division is probably not related to core cell cycle activity. This hypothesis is supported by the observation that no core cell cycle genes were DE in the microarray experiment using shoot apices of *elo* mutants.

Molecular Phenotyping. We studied the molecular phenotype to assess whether the same sets of genes were DE in the mutants. To distinguish the DE genes that were not a direct consequence of the *elo* and *drl* mutations but were, rather, a secondary effect of the leaf phenotype, another narrow leaf mutant, *angusta4* (*ang4*) (12), was included as a control. The analysis of 2609 cDNA-AFLP transcripts derived from the seven genotypes (*Ler*, *elo1*, *elo2*, *elo3*, *elo4/drl1-4*, *drl1-2*, and *ang4*) showed that 763 (29%) transcripts were DE in the mutants and the wild type (at $P \leq 0.001$). These 763 DE transcripts were used for clustering to observe the distances between the genome expression profiles of mutants. The clustering result showed clearly that *ang4* was distant from the *elongata* genotypes, which, in turn, clustered together, but were divided into two subgroups: *drl1-2*, *elo4/drl1-4* (the two alleles of *DRL1*), and *elo3* in one group, which comprises mutants in a regulator and the key enzyme of the complex, and *elo1* and *elo2* in a second group, whose respective genes are involved in Elongator architecture (Fig. 2G).

A genome-wide analysis with the Affymetrix ATH1 microarrays on *elo2*, *elo3*, *drl1-2*, and *ang4* mutants identified a total number of 2,897 genes that were DE in at least one mutant and

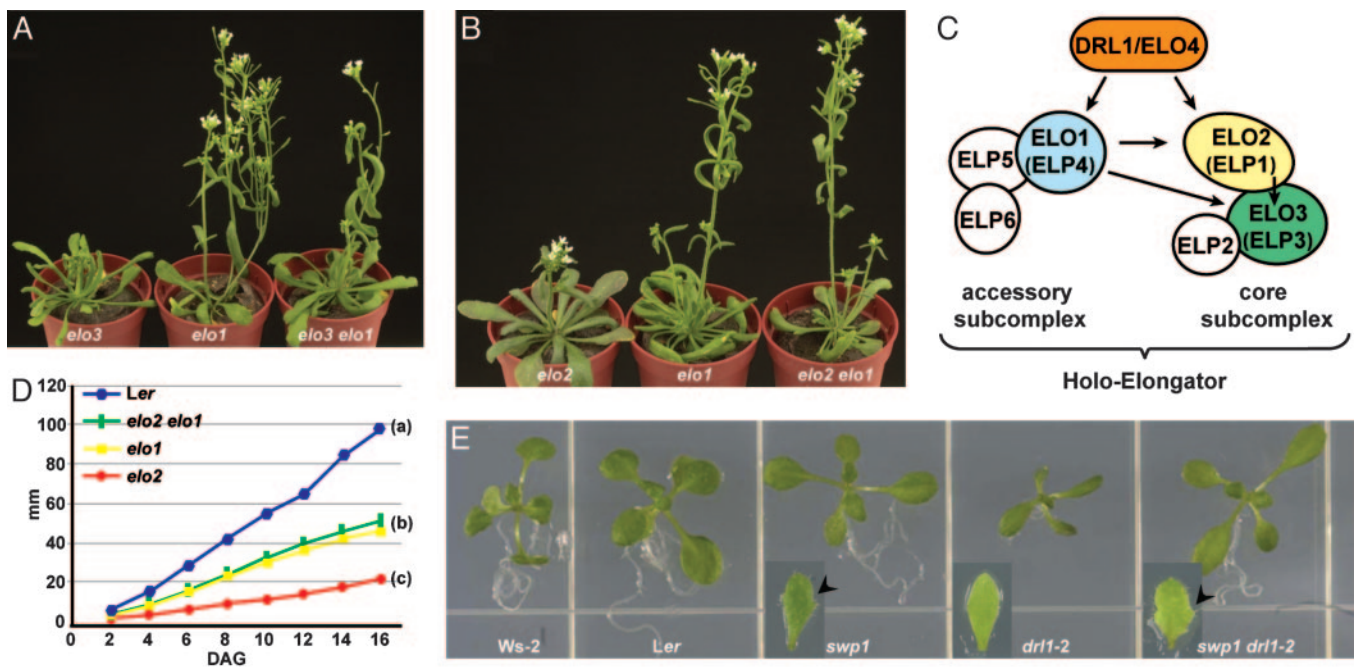


Fig. 3. DM analysis. (A and B) Inflorescences of the *elo3 elo1* (A) and *elo2 elo1* (B) DM and their parents (40 DAG). (C) Schematic overview of the composition of the Elongator complex in yeast (according to ref. 4). The arrows indicate the epistatic interactions from the DM analysis in *Arabidopsis*, starting from the epistatic gene. (D) Primary root growth kinetics of *elo1*, *elo2*, *elo2 elo1*, and *Ler*. A pairwise multiple-testing analysis positioned the lines in groups a to c. (E) DM analysis between *swp1* and *drl1-2*. The *swp1 drl1-2* DMs are shown together, with the parents and the wild types, *Ws-2* and *Ler*, as controls. Details of the leaf serrations (indicated with an arrow) of the third leaf (21 DAG) are shown for the mutants.

the wild type (at $P \leq 0.05$). In the cluster tree observed from this set of genes, also *elo2*, *elo3*, and *drl1-2* belonged to the same group distant from *ang4* (Fig. 2G). Thus, the genome expression profiles of the Elongator mutants indicate that the mutations in the *ELO2*, *ELO3*, *ELO1*, and *DRL1* genes affect the transcriptome similarly. The analogous molecular processes affected by mutations in the *ELO* and *DRL1* genes provide additional experimental evidence for their function in a complex.

Genetic Interactions Between the Different Elongator Genes. The different *elo* and *drl* homozygotes were crossed to obtain *elo2 elo1*, *elo2 drl1-2*, *elo4 elo1*, *elo3 elo1*, and *elo3 elo2* DMs. The F_1 progeny of each cross was phenotypically wild-type, and no new phenotype was found in the F_2 population. The cleaved amplified polymorphic sequence technique (23) was used to distinguish *elo1*, *elo2*, *elo3*, and *elo4/drl1-4* mutant alleles from their corresponding wild-type alleles in F_2 putative DMs. A PCR analysis with a *Dissociation* primer (14) in combination with *DRL1* gene-specific primers was performed to identify the *drl1-2* homozygotes. Two *elo4 elo1*, three *elo2 elo1*, four *elo2 drl1-2*, one *elo3 elo1*, and three *elo3 elo2* DMs were identified by this analysis. All DMs had a narrow leaf phenotype similar to that of the respective parents (Fig. 6, which is published as supporting information on the PNAS web site), indicating that *ELO2*, *ELO3*, *ELO1*, and *DRL1* act in the same process. Moreover, these observations suggest complex formation because they placed proteins whose yeast homologs were shown to belong to two subcomplexes or to function as a regulator, together in one process. The differences in the rosette leaf phenotype are subtle among the various *elo* and *drl* mutants and, therefore, this phenotypic trait could not be used to determine epistasis among the Elongator genes without extensive microscopic analysis in contrast to growth of the primary root and architecture of the inflorescence that allowed a clear distinction between some of the *elo* and *drl* mutants. Two cases are exemplified in Fig. 3: *elo3 elo1* and *elo2 elo1*, whose DMs exhibit a root and inflorescence

phenotype similar to that of the less dramatic parent, *elo1*. A pairwise statistical analysis was performed on the root growth and positioned the DMs in the same group as *elo1*, distant from *elo2* and *elo3* (Fig. 3D); also, the architecture of the DM inflorescences was less dramatically affected and similar to that of the *elo1* mutant (Fig. 3A and B). The other DM combinations were also phenotypically characterized and compared with their respective parents. The *elo2 elo3*, *elo4 elo1*, and *elo2 drl1-2* DMs had phenotypes similar to those of *elo2*, *elo4/drl1-4*, and *drl1-2*, respectively. Thus, *DRL1* was epistatic to *ELO2* and *ELO1*. Because the corresponding proteins have been shown to be part of distinct subcomplexes of Elongator in yeast, this observation is in accordance with a proposed role for *DRL1* as a regulator of the holocomplex (15). Furthermore, *ELO1* was epistatic over *ELO2* and *ELO3*, indicating the importance of the accessory subcomplex for the function of the core subcomplex. Finally, *ELO2* was epistatic to *ELO3*, suggesting that the *ELO2* scaffold protein is important for the maintenance of the integrity of Elongator as a HAT complex. These epistasis data can be correlated with the proposed functions of the proteins in *Arabidopsis* as well as with the model proposed in yeast for the Elongator complex formation (Fig. 3C) (4).

Genetic Interactions Between *SWP1* and *DRL1*. The *struwwelpeter1* (*swp1*) recessive mutation, which was isolated in a *Ws-2* background, also causes narrow leaves with a reduced cell number. The *SWP1* gene encodes a component of the Mediator complex that associates with the RNAPII transcription initiation complex (17). A *SWP1/swp1* \times *drl1-2/drl1-2* cross was performed, of which the F_1 plants were selected on phosphinothricin, the marker present on the T-DNA inducing the *swp1* mutation, to select F_1 plants that contained the *swp1* mutation. All plants that survived this selection displayed a wild-type phenotype. In the F_2 population, no novel or additive phenotype could be detected; so, the mutant plants from this population were analyzed molecularly by PCR to identify *drl1-2* homozygotes. From these

plants, the F_3 seeds were grown selectively on phosphinothricin, and the 100% resistant lines were identified as *swp1 drl1-2* DMs. All individuals from two DM lines had a phenotype similar to that of the *swp1* mutants: no growth retardation, small serrations in the first leaves, and normal growth of the primary root and inflorescence (Fig. 3E), indicating that *SWPI* is epistatic to *DRL1*. These genetic data position Elongator more downstream in the RNAPII-mediated transcription process than Mediator in the plant system, which is consistent with the role of the yeast Elongator complex in transcription elongation.

Conclusion

We demonstrated that the Elongator complex is present in plants and that the functional domains of three component proteins are conserved. Several lines of evidence also suggest complex formation in plants, indicating that Elongator is structurally conserved. By positioning the Elongator complex in the process of RNAPII-mediated transcription, downstream of Mediator, we showed that the function of the complex is conserved.

Although the Elongator complex is very well conserved, the phenotypes of the Elongator mutant plants show that its function differs in unicellular and multicellular organisms. In yeast, Elongator mutants are retarded in growth because of a slow adaptation to changing environmental conditions (40). However, in plants, the disruption of the Elongator complex has effects throughout development: germination, vegetative growth, and the reproductive phase were affected in the mutants. In humans, the Elongator complex also plays a role in development, as a mutation in one of the Elongator components is associated with the neuronal syndrome, familial dysautonomia (41). This neurodevelopmental genetic disorder affects devel-

opment and maintenance of sensory and autonomic neurons, resulting in a wide range of pathologies primarily due to malperception of stimuli from the environment and during development (42).

In addition, the analysis of the plant Elongator mutants revealed that the Elongator complex has a positive effect on the cell proliferation rate during organ growth, without affecting the core cell cycle machinery. Our data indicate that the mechanism by which the Elongator complex affects the cell division rate is different in yeast and higher plants. The identification of the Elongator complex in plants now offers opportunities to gain more insights into the role of the Elongator complex in multicellular organisms. Because plants are easily amenable to experimentation, it will be possible to determine the environmental and developmental cues that direct Elongator activity and the molecular processes regulated by this complex. The microarray experiments revealed that only a limited number of processes are affected in the *elo* and *drl* mutants, i.e., secondary metabolism, photomorphogenesis, and several stress responses, indicating that Elongator selectively influences transcriptional activity. The mechanism behind these selective roles of Elongator will need to be explored further.

We thank Gerda Cnops, Andrea Falcone, Sabine De Block, Els Van Der Schueren, Wilson Ardiles-Diaz, Olivier Grandjean, Paul Van Hummelen, and Gerrit T. S. Beemster for technical help or expertise and Martine De Cock for help in preparing the manuscript. The work was supported by European Research Training Network HPRN-CT-2002-00267 (DAGOLIGN), a fellowship from the Instituut voor de Aanmoediging van Innovatie door Wetenschap en Technologie in Flanders (to H.N.), and Marie Curie Training Site Fellowships QLK3-GH-01-60058-02 (to H.N.) and HPMT-CT-2000-00088 (to L.B.).

- Jenuwein, T. & Allis, C. D. (2001) *Science* **293**, 1074–1080.
- Loidl, P. (2004) *Trends Plant Sci.* **9**, 84–90.
- Gregory, P. D., Wagner, K. & Hörz, W. (2001) *Exp. Cell Res.* **265**, 195–202.
- Fichtner, L., Frohloff, F., Jablonowski, D., Stark, M. J. R. & Schaffrath, R. (2002) *Mol. Microbiol.* **45**, 817–826.
- Otero, G., Fellows, J., Li, Y., de Bizemont, T., Dirac, A. M. G., Gustafsson, C. M., Erdjument-Bromage, H., Tempst, P. & Svejstrup, J. Q. (1999) *Mol. Cell* **3**, 109–118.
- Hawkes, N. A., Otero, G., Winkler, G. S., Marshall, N., Dahmpus, M. E., Krappmann, D., Scheiderei, C., Thomas, C. L., Schiavo, G., Erdjument-Bromage, H., et al. (2002) *J. Biol. Chem.* **277**, 3047–3052.
- Pandey, R., Muller, A., Napoli, C. A., Selinger, D. A., Pikaard, C. S., Richards, E. J., Bender, J., Mount, D. W. & Jorgensen, R. A. (2002) *Nucleic Acids Res.* **30**, 5036–5055.
- Tian, L. & Chen, Z. J. (2001) *Proc. Natl. Acad. Sci. USA* **98**, 200–205.
- Vlachonasiou, K. E., Thomashow, M. F. & Triezenberg, S. J. (2003) *Plant Cell* **15**, 626–638.
- He, Y., Michaels, S. D. & Amasino, R. M. (2003) *Science* **302**, 1751–1754.
- Zhou, C., Labbe, H., Sridha, S., Wang, L., Tian, L., Latoszek-Green, M., Yang, Z., Brown, D., Miki, B. & Wu, K. (2004) *Plant J.* **38**, 715–724.
- Berná, G., Robles, P. & Micol, J. L. (1999) *Genetics* **152**, 729–742.
- Robles, P. & Micol, J. L. (2001) *Mol. Genet. Genomics* **266**, 12–19.
- Nelissen, H., Clarke, J. H., De Block, M., De Block, S., Vanderhaeghen, R., Zielinski, R. E., Dyer, T., Lust, S., Inzé, D. & Van Lijsebettens, M. (2003) *Plant Cell* **15**, 639–654.
- Fichtner, L., Frohloff, F., Bürkner, K., Larsen, M., Breunig, K. D. & Schaffrath, R. (2002) *Mol. Microbiol.* **43**, 783–791.
- Autran, D., Jonak, C., Belcram, K., Beemster, G. T. S., Kronenberger, J., Grandjean, O., Inzé, D. & Traas, J. (2002) *EMBO J.* **21**, 6036–6049.
- Bechtold, N., Ellis, J. & Pelletier, G. (1993) *C. R. Acad. Sci.* **316**, 1194–1199.
- Cnops, G., Jover-Gil, S., Peters, J. L., Neyt, P., De Block, S., Robles, P., Ponce, M. R., Gerats, T., Micol, J. L. & Van Lijsebettens, M. (2004) *J. Exp. Bot.* **55**, 1529–1539.
- Laufs, P., Dockx, J., Kronenberger, J. & Traas, J. (1998) *Development (Cambridge, U.K.)* **125**, 1253–1260.
- Boyes, D. C., Zayed, A. M., Ascenzi, R., McCaskill, A. J., Hoffman, N. E., Davis, K. R. & Görlach, J. (2001) *Plant Cell* **13**, 1499–1510.
- Beemster, G. T. S., De Veylder, L., Vercautse, S., West, G., Rombaut, D., Van Hummelen, P., Galichet, A., Gruissem, W., Inzé, D. & Vuylsteke, M. (2005) *Plant Physiol.* **10.1104/pp.104.053884**.
- De Veylder, L., Beeckman, T., Beemster, G. T. S., Krols, L., Terras, F., Landrieu, I., Van Der Schueren, E., Maes, S., Naudts, M. & Inzé, D. (2001) *Plant Cell* **13**, 1653–1667.
- Neff, M. M., Neff, J. D., Chory, J. & Pepper, A. E. (1998) *Plant J.* **14**, 387–392.
- Neff, M. M., Turk, E. & Kalishman, M. (2002) *Trends Genet.* **18**, 613–615.
- Breynne, P., Dreesen, R., Vandepoele, K., De Veylder, L., Van Breusegem, F., Callewaert, L., Rombauts, S., Raes, J., Cannoot, B., Engler, G., et al. (2002) *Proc. Natl. Acad. Sci. USA* **99**, 14825–14830.
- Gautier, L., Cope, L., Bolstad, B. M. & Irazary, R. A. (2004) *Bioinformatics* **20**, 307–315.
- Lönnstedt, I. & Speed, T. (2002) *Stat. Sin.* **12**, 31–46.
- Eisen, M. B., Spellman, P. T., Brown, P. O. & Botstein, D. (1998) *Proc. Natl. Acad. Sci. USA* **95**, 14863–14868.
- Alonso, J. M., Stepanova, A. N., Leisse, T. J., Kim, C. J., Chen, H., Shinn, P., Stevenson, D. K., Zimmerman, J., Barajas, P., Cheuk, R., et al. (2003) *Science* **301**, 653–657.
- Wittschieben, B. Ø., Otero, G., de Bizemont, T., Fellows, J., Erdjument-Bromage, H., Ohba, R., Li, Y., Allis, C. D., Tempst, P. & Svejstrup, J. Q. (1999) *Mol. Cell* **4**, 123–128.
- Chinenov, Y. (2002) *Trends Biochem. Sci.* **27**, 115–117.
- Ponting, C. P. (2002) *Nucleic Acids Res.* **30**, 3643–3652.
- Rashid, N., Morikawa, M. & Imanaka, T. (1996) *Mol. Gen. Genet.* **253**, 397–400.
- Zimmermann, P., Hirsch-Hoffmann, M., Hennig, L. & Gruissem, W. (2004) *Plant Physiol.* **136**, 2621–2632.
- Clark, S. E., Running, M. P. & Meyerowitz, E. M. (1993) *Development (Cambridge, U.K.)* **119**, 397–418.
- Fichtner, L. & Schaffrath, R. (2002) *Mol. Microbiol.* **44**, 865–875.
- Brown, R. (1951) *J. Exp. Bot.* **2**, 96–110.
- De Veylder, L., Beeckman, T., Beemster, G. T. S., de Almeida Engler, J., Ormenese, S., Maes, S., Naudts, M., Van Der Schueren, E., Jacquard, A., Engler, G. & Inzé, D. (2002) *EMBO J.* **21**, 1360–1368.
- Wyrzykowska, J., Pien, S., Shen, W. H. & Fleming, A. J. (2002) *Development (Cambridge, U.K.)* **129**, 957–964.
- Frohloff, F., Fichtner, L., Jablonowski, D., Breunig, K. D. & Schaffrath, R. (2001) *EMBO J.* **20**, 1993–2003.
- Slaugenhaupt, S. A. & Gusella, J. F. (2002) *Curr. Opin. Genet. Dev.* **12**, 307–311.
- Axelrod, F. B. (2004) *Muscle Nerve* **29**, 352–363.